3

miR-25 modulates invasiveness and dissemination of human prostate cancer cells via regulation of α_v- and α_6 integrin expression

Eugenio Zoni
Geertje van der Horst
Marjan van de Merbel
Lanpeng Chen
Jayant K. Rane
Rob C.M. Pelger
Anne T. Collins
Tapio Visakorpi
Ewa B. Snaar-Jagalska
Norman J. Maitland
Gabri van der Pluijm

Cancer Research 2015 Jun 1;75(11):2326-36.

Abstract

Altered microRNA (miR) expression is associated with tumor formation and progression of various solid cancers. A major challenge in miR expression profiling of bulk tumors is represented by the heterogeneity of the subpopulations of cells that constitute the organ, as well as the tumor tissue. Here we analyzed the expression of miRs in a subpopulation of epithelial stem/progenitor-like cells in human prostate cancer (PCSC) and compared their expression profile to more differentiated cancer cells. In both cell lines and clinical prostate cancer specimens we identified that miR-25 expression in PCSCs was low/absent and steadily increased during their differentiation into cells with a luminal epithelial phenotype. Functional studies revealed that overexpression of miR-25 in prostate cancer cell lines and selected subpopulation of highly metastatic and tumorigenic cells ($ALDH^{high}$) strongly affected the invasive cytoskeleton causing reduced migration *in vitro* and metastasis via attenuation of extravasation *in vivo*. Here we show, for the first time, that miR-25 can act as a tumor suppressor in highly metastatic PCSCs by direct functional interaction with the 3'UTR of pro-invasive α_v- and α_6 integrins. Taken together, our observations suggest that miR-25 is a key regulator of invasiveness in human prostate cancer through its direct interactions with α_v- and α_6 integrin expression.

Introduction

Prostate cancer is the second most frequently diagnosed cancer and the sixth leading cause of death from cancer in males worldwide (1). Despite the progress in the pathogenesis, detection, and treatment of primary tumor, the main problem for prostate cancer patients remains the risk of metastasis formation and tumor recurrence after surgical removal and/or treatment of the primary tumor.

From a hierarchical point of view, normal and transformed epithelial tissues are indeed characterized by a cellular heterogeneity, in which different cell types contribute to the maintenance of the complexity of tissues (2). One of the major challenges in the field of new therapy development for advanced cancer is to specifically target “driver” cancer cell subpopulations, that seem to be involved in tumor maintenance, metastasis and therapy resistance (3). Accumulating evidence shows that prostate cancer stem/progenitor-like cells play key roles in tumor initiation, local and distant relapse, metastasis, and castration- & chemotherapy resistance (4,5). One of the driving forces of oncological transformation of normal epithelial stem cells (SC) into cancer stem cells (CSCs), is the deregulated gene expression of tumor suppressors and oncogenes (6). Furthermore, oncological research has highlighted an emerging role for microRNAs (miRs) as crucial regulators of such oncogenes and tumor suppressors in cancer (7). miRs are a class of small non-coding RNA molecules (18-25 nucleotides long), which modulate gene expression by binding to the 3’-untranslated regions (3’-UTR) of target mRNAs and promoting mRNA degradation or translational repression (8). Several studies have delineated and compared the expression of miRs in bulk tissues from human prostate cancer and normal prostate and have shown significant correlations between miRs levels, prostate cancer progression and response to chemotherapy (9,10). In addition, these studies have highlighted the diagnostic and prognostic value of miRs detection in blood and urine, suggesting the possible relevance of the use of miRs as prostate cancer biomarkers.

Most attempts to decipher the miRs signatures have been performed in clinical samples of bulk tumor tissues or heterogeneous prostate cancer cell lines. In these heterotypic and heterogeneous cell populations, this strategy cannot clearly discriminate between the “driver” subpopulation and other, non-tumorigenic and more differentiated cancer cell subpopulations. In bulk tumor tissues, it is even more difficult to discriminate between tumor-derived and stroma-derived miR expression profiles.

Here we examined the expression of miRs in the “driver” subpopulation of human stem/progenitor-like prostate cancer cells (cell lines, patient samples) that was previously shown to drive tumorigenesis and metastasis in preclinical prostate cancer models of bone metastasis *in vivo* (11). Based on the list of differentially expressed miRs,

miR-25 was selected because a number of its putative target genes are predicted to be involved in the stimulation of cancer invasiveness. In both clinical prostate cancer specimens and prostate cancer cell lines we found that miR-25 is low/absent in the $\alpha 2\beta 1^{hi}$ /$CD133^{+}$ compartment, also referred to as stem-like cells (SC) in recent publication (12). and steadily increases during differentiation into luminal epithelial cells in clinical samples. Here we validate, for the first time, the direct functional interaction between miR-25 and α_v- and α_6 integrins linked to the cytoskeletal organization and invasive behavior *in vitro*. In line with these observations, we further demonstrate that miR-25 targeted α_v- and α_6 integrins in selected $ALDH^{high}$ subpopulation of cancer stem/progenitor cells and reduced invasion by blocking the extravasation of human prostate cancer cells in the intact organism.

Materials and Methods

ALDEFLUOR® assay and real time PCR-based microRNA expression profiling

Aldehyde Dehydrogenase (ALDH) activity of the cells was measured using the ALDEFLUOR® assay kit (StemCell Technologies, Durham, USA) according to the manufacturer's protocol (11). ALDH substrate was added to the cells and converted by intracellular ALDH into a fluorescent product. For FACS sorting cells were labelled with ALDEFLUOR® kit and sorted using FACS ARIA cell sorter (BD Bioscience, Breda, The Netherlands) ($ALDH^{high}$ = highest 10% $ALDH^{+}$; $ALDH^{low}$ = lowest 10% $ALDH^{-}$ cells). microRNA expression profiling was performed using RT^2 miRNA PCR array (SA-biosciences, Frederick, USA) according to the manufacturer's protocol. Data were normalized using SNORD48 and U6 RNA housekeeping genes. Inclusion criteria were Ct value <35, fold induction >2 and <-2 and similar data in 2 independent experiments.

Prostate cancer cell lines and transfection with miR-25 precursor molecule

Human osteotropic prostate cancer cell lines PC-3M-Pro4Luc2 and C4-2B cells were maintained in DMEM with 10% FCII, 1% Penicillin-Streptomycin (Life Technologies, USA) and 0.8 mg/ml Neomycin (Santacruz, USA) and T-medium DMEM (Sigma-Aldrich, The Netherlands) with 20% F-12K nutrient mixture Kaighn's modification (GibcoBRL), 10% FCS, 1% Insulin-Transferin-Selenium, 0.125 mg/ml biotin, 12.5 mg/ml adenine, 6.825 ng/ml T3 and 1% penicillin/streptomycin respectively. Cells were maintained at 37°C with 5% CO_2.

For transient transfection, Lipofectamine® 2000 (Invitrogen, USA) was used according to manufacturer's protocol with Pre-miR-25 (ID: PM10584; Life Technologies) and pre-miRNA negative control (scramble) (ID: AM17110; Life Technologies). Total RNA was collected after 72 hours.

Collection of samples from patient, isolation of subpopulation from primary prostate epithelial cells and expression array

Prostate epithelial tissue was collected with ethical permission from York District Hospital (York) and Castle Hill Hospital (Cottingham, Hull). Primary epithelial prostate cells were expended in culture and selected for $\alpha_2\beta_1$ integrin expression using rapid adhesion to type collagen-I coated plates (13). $\alpha_2\beta_1^{hi}$ cells were subsequently enriched for $CD133^{-}$ and $CD133^{+}$ fraction using MACS cell sorting according to the manufacturer's protocol (Milteny Biotec) (5,12,14). Cultured cells were harvested at passage 2 and total RNA was extracted using miRVana kit (Life Technology, Paisley, UK). Agilent V3 arrays

were used to perform miR microarray analysis and the data was processed using Agilent Feature extraction software. The data were quantile normalized, and RMA summarized.

miRNA target prediction and bioinformatic analysis of cluster of genes

Targetscan v6.2, miRDB (15) and microT-CDS (16) were used to identify novel miR-25 predicted targets. Functional annotation was performed using DAVID Bioinformatics Resources 6.7 (17,18) and KEGG database (19).

RNA isolation and real-time qPCR

Total RNA was isolated using Trizol (Invitrogen, USA), cDNA was synthesized by reverse transcription (Promega, USA) according to manufacturer's protocol and qRT-PCR performed with Biorad CFX96 system (Biorad, The Netherlands). Expression was normalized to GAPDH. (Primer sequences in **supplementary table I**).

Migration assay

Cells were starved overnight in medium containing 0.3% serum and then seeded in medium containing 0.3% serum in Transwell chamber (Corning 8-µm pore size). The lower chamber was filled with medium containing 10% serum. After 18 hours of incubation, cells on the upper side of the filters were removed and cells migrated to the lower side were fixed with 4% paraformaldehyde, stained with 0.1% crystal violet (Sigma-Aldrich, USA) and counted.

Proliferation assay

Cells were seeded at density of 2,000 cells/well 24 hours and allowed to grow for 24, 48, 72. After incubation, 20 µl of 3-(4,5 dimethylthiazol-2-yl)-5-(3-carboxymethoxyphenyl)-2-(4-sulfophenyl)-2H-tetrazolium was added and mitochondrial activity was measured after 2 hours incubation at 37°C. (CellTiter96 Aqueous Non-radioactive Cell proliferation assay, Promega, USA).

FACS analysis

Protein expression was measured with flow-cytometry. 1 x 10^5 cells were incubated for 45 min at 4°C in FACS wash buffer containing PBS + 1% FCS + 0.1% Natriumazide NaN_3 and 10 µl antibody (αV-PE, α2-FITC, α6-APC, Milteny). Cells were washed with PBS, protein measured with FACS Calibur (BD Biosciences, USA) and data analysed with FCS express software™ (De Novo software, USA).

Phalloidin staining

PC-3M-Pro4luc2 transfected with Pre-miR-25 and scramble negative control were seeded onto glass slides, fixed with 4% paraformaldehyde and stained with 0.25 μM Phalloidin (Life technologies, USA). TOPRO (Life technologies) was used for nuclei visualization. Images were acquired with confocal microscope leica SP5 (Leica, Germany) and analysed with ImageJ (NIH).

Reporter constructs and luciferase assay

497 bp and 485 bp nucleotide sequences corresponding to portion of the 3' UTR of ITGA6 and ITGAV respectively, including the conserved predicted binding site (seed sequence) for miR-25 were cloned downstream of the *firefly* Luciferase2 sequence in a PGL4.10 vector (Promega, USA) using XbaI (Promega) and FseI (New England Biolabs, USA) restriction enzymes. 1184 bp sequence of human elongation factor 1α (hEF1α) promoter was inserted into the multiple cloning site (MCS) of the PGL4.10 upstream the luciferase2 sequence using KpnI and HindIII (Promega). Mutagenesis was performed using QuikChange® (Stratagene, USA) site-directed mutagenesis approach. (Primer sequences in **supplementary table II**).

Zebrafish maintenance

Tg(mpo:GFP)i114 zebrafish line (20,21) was handled compliant to local animal welfare regulations and maintained according to standard protocols (www.ZFIN.org).

Zebrafish embryo preparation and tumor cell implantation

2 days-post fertilisation (dpf) dechorionized zebrafish embryos were anaesthetized with 0.003% tricaine (Sigma) and placed on a 10-cm Petridish coated with 3% agarose. PC-3M-Pro4mCherry cells were transfected 48h before implantation. Single cell suspensions were re-suspended in PBS, kept at room temperature before implantation and implanted within 3 h. The cell suspension was loaded into borosilicate glass capillary needles (1 mm O.D. × 0.78 mm I.D.; Harvard Apparatus) and the injections were performed using a Pneumatic Picopump and a manipulator (WPI, UK). Approximately 400 cells were injected at around 60 μm above the ventral end of the duct of Cuvier (DoC), where the DoC opens into the heart. After implantation with mammalian cells, zebrafish embryos (including non-implanted controls) were maintained at 33°C, to compromise between the optimal temperature requirements for fish and mammalian cells (22). Data are representative of at least two independent experiments with at least fifty embryos per group. Experiments were discarded when the survival rate of the control group was less than 80%.

Statistical analysis

Statistical analysis was performed with GraphPad Prism 6.0 (GraphPad software) using t-test for comparison between two groups. Data is presented as mean ± SEM. P-values ≤ 0.05 were considered to be statistically significant (* $P < 0.05$, ** $P < 0.01$, *** $P < 0.001$).

Results

miR-25 expression is down-regulated in normal and transformed prostate stem cells (PCSC) and steadily increases upon luminal differentiation.

To investigate the expression of miRs in prostate cancer stem cells (PCSCs), we used the ALDEFLUOR assay, which involves viable cell sorting based on ALDH enzyme activity (23,24). After viable sorting ALDH^{high} and ALDH^{low} subpopulations of PC-3M-Pro4Luc2 were used to identify the differential miR expression profiles of cancer stem cells (ALDH^{high}) and committed non-tumorigenic & non-metastatic (ALDH^{low}) cells (11). Real Time PCR-based miR expression profiling revealed that miR-25 was the most down-regulated microRNA in cancer stem cells (ALDH^{high}) compared to ALDH^{low} subpopulation of cells (LOG10-Fold change -2,76 p-value=0,05). (**Fig. 1A**).

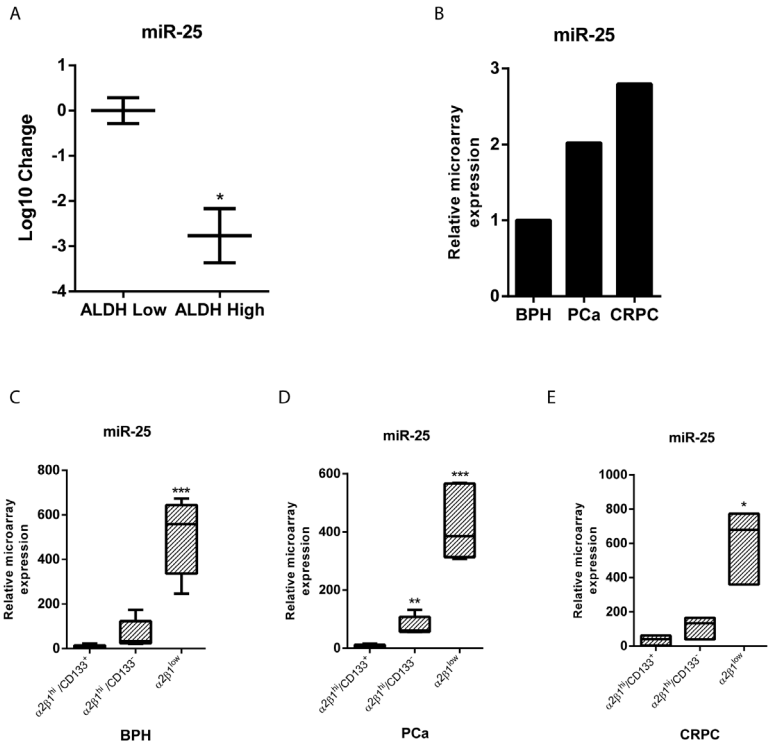

Figure 1. Differential expression of miR-25 in prostate cancer, prostate cancer stem-like cells, and benign prostate epithelial stem cells. A) miR-25 expression in ALDH^{high} versus ALDH^{low} subpopulation isolated from PC-3M-Pro4Luc2 cells measured with real time PCR-based miRNA expression profiling; error bars, ±SEM (n = 2). **B**) relative array expression of miR-25 in BPH, PCa (prostate cancer), and CRPC samples isolated from patients. **C**) relative array expression of miR-25 in α2β1hi/CD133+,

α2β1hi/CD133−, and α2β1low compartment, also referred to as stem-like cells, TA cells, and CB cells, respectively (12), isolated from BPH (n = 5 patients), PCa (prostate cancer; n = 5 patients; **D**), and CRPC (n = 3 patients; **E**); error bars, ±SEM. *, P < 0.05; **, P < 0.01; ***, P < 0.001.

We next investigated miR expression in subpopulations isolated from prostate tissue and primary epithelial cultures derived from patients with Benign Prostatic Hyperplasia (BPH), hormone-naïve prostate cancer (PCa, > Gleason 7) and castration-resistant prostate cancer (CRPC) (12). First we quantified the expression of miR-25 in unfractionated soft tissue collected from BPH, PCa and CRPC and found increased miR-25 expression upon tumor progression. (**Fig. 1B**). Then, after expansion of primary prostate cells in culture, we compared miR-25 expression in three cell populations: $\alpha2\beta1^{hi}$ /$CD133^{+}$, $\alpha2\beta1^{hi}$ /$CD133^{-}$, and $\alpha2\beta1^{low}$, also referred to as stem-like cells (SC), transit amplifying cells (TA) and committed basal cells (CB), respectively (5,12,14,25). Interestingly, miR-25 is significantly and strongly down-regulated in the $\alpha2\beta1^{hi}$ /$CD133^{+}$ population compared to the $\alpha2\beta1^{hi}$ /$CD133^{-}$ and $\alpha2\beta1^{low}$ compartments, irrespective of their pathological status (i.e. BPH, PCa and CRPC) (**Fig. 1C, D, E**).
Taken together, our data show consistent relative low expression levels of miR-25 in the cancer stem/progenitor subpopulation of cells in both human prostate cancer cell lines and the compartment defined as $\alpha2\beta1^{hi}$ /$CD133^{+}$ cells isolated from prostate cancer patients (12,25). The expression of miR-25 steadily and consistently increases during epithelial differentiation in patient-derived benign prostates (BPH) and malignant prostate samples.

Identification and transcriptional analysis of miR-25 predicted target genes.

Next Targetscan (Release 6.2) was used to identify novel miR-25 predicted target genes (26). Using this approach we identified 893 conserved putative target genes, with a total of 992 conserved sites and 211 poorly conserved sites. Among the list of predicted targets, 63 genes were mapped, using the database for annotation, visualization and integrated discovery DAVID (17,18), in processes linked to invasion and pathways related to prostate cancer and bone metastasis (Regulation of f-actin cystoskeleton, ECM-receptor interaction, TGF-β signalling pathway, MAPK signalling pathway and cell cycle). Interestingly, our *in silico* analysis showed that the regulation of F-actin cytoskeleton was one of the predicted pathways that is potentially affected by miR-25 (p-value = 2.1E-2). Mapping of the predicted miR targets to the regulation of F-actin cytoskeleton, KEGG pathway identified multiple genes involved in important processes for cell motility, migration, invasion and cytoskeleton dynamic. (**Fig. 2A**).

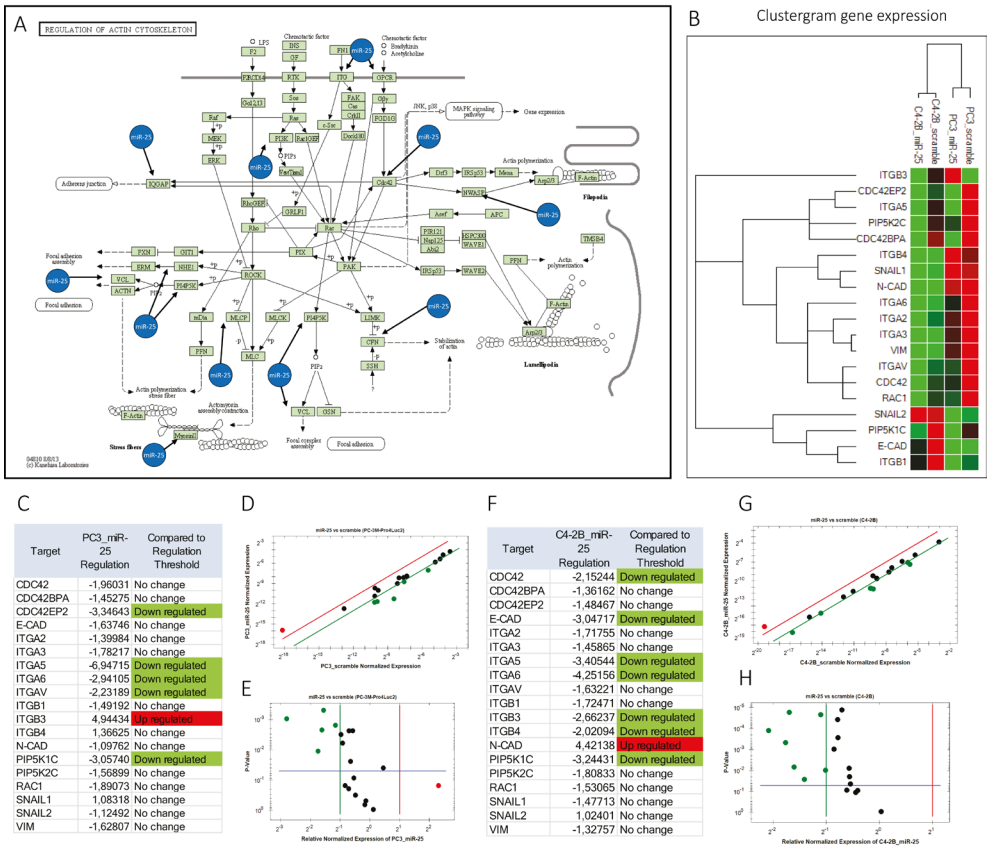

Target	PC3_miR-25 Regulation	Compared to Regulation Threshold
CDC42	-1,96031	No change
CDC42BPA	-1,45275	No change
CDC42EP2	-3,34643	Down regulated
E-CAD	-1,63746	No change
ITGA2	-1,39984	No change
ITGA3	-1,78217	No change
ITGA5	-6,94715	Down regulated
ITGA6	-2,94105	Down regulated
ITGAV	-2,23189	Down regulated
ITGB1	-1,49192	No change
ITGB3	4,94434	Up regulated
ITGB4	1,36625	No change
N-CAD	-1,09762	No change
PIP5K1C	-3,05740	Down regulated
PIP5K2C	-1,56899	No change
RAC1	-1,89073	No change
SNAIL1	1,08318	No change
SNAIL2	-1,12492	No change
VIM	-1,62807	No change

Target	C4-2B_miR-25 Regulation	Compared to Regulation Threshold
CDC42	-2,15244	Down regulated
CDC42BPA	-1,36162	No change
CDC42EP2	-1,48467	No change
E-CAD	-3,04717	Down regulated
ITGA2	-1,71755	No change
ITGA3	-1,45865	No change
ITGA5	-3,40544	Down regulated
ITGA6	-4,25156	Down regulated
ITGAV	-1,63221	No change
ITGB1	-1,72471	No change
ITGB3	-2,66237	Down regulated
ITGB4	-2,02094	Down regulated
N-CAD	4,42138	Up regulated
PIP5K1C	-3,24431	Down regulated
PIP5K2C	-1,80833	No change
RAC1	-1,53065	No change
SNAIL1	-1,47713	No change
SNAIL2	1,02401	No change
VIM	-1,32757	No change

Figure 2. In silico analysis for predicted pathway identification and validation by RT-qPCR. A) interaction between miR-25 and predicted target genes overlaid on KEGG regulation of the actin cytoskeleton pathway. **B**) clustergram of mRNA expression assessed by RT-qPCR for selected target among those represented in A. Analysis performed in PC-3M-Pro4Luc2 and C4-2B cells (N = 3). Colors match with those represented in B, D, E, F, G, H (green, downregulation; red, upregulation). **C**) mRNA regulation of selected target genes on PC-3M-Pro4Luc2–overexpressing miR-25; regulation is highlighted in green (down) and red (up). Colors are matched with scatter plot (**D**) with threshold selected (threshold value = 2) and significant values are represented in volcano plot (**E**). **F**) mRNA regulation of selected target genes on C4-2B–overexpressing miR-25; regulation is highlighted in green (down) and red (up). Colors are matched with scatter plot (**G**) with threshold selected (threshold value = 2) and significant values are represented in volcano plot (**H**).

Strikingly, miR-25 was predicted to target IQGAP2 (a GTP-dependent protein involved in the cytoskeletal reorganization), WASL and CFL2 (involved in the actin polymerization and depolymerization), CDC42 (required for rounded/ameboid movements of single tumor cells), MYH9 (cellular myosin with a role in cytokinesis and cell shape), PIP4K2C and PIP5K1C (kinase which mediates RAC1-dependent reorganization of actin filaments

(27)). RAC1 is involved in focal adhesion and is required for mesenchymal movements of single tumor cells (28)), PIKFYVE (which plays a role in endosome-related membrane trafficking), PPP1R12A (regulates myosin phosphatase activity), SLC9A1 (sodium/hydrogen exchanger involved in focal adhesion), ITGA5 (a.k.a. fibronectin receptor, significantly down-regulated by miR-25 in both cell lines as shown by qRT-PCR analysis **(Fig. 2 B,C,D,E and Fig. 2 F,G,H)**) and ITGAV (a.k.a. vitronectin receptor), ITGA6 (laminin-10/11 receptor) and Vinculin (VCL, however not affected by miR-25 as shown by western blot **(Suppl. Fig. 1A)** that are all involved in cell-matrix interactions and adhesion. Among the target genes involved in the regulation of the F-actin cytoskeleton, ITGAV and ITGA6 are members of the integrin family of transmembrane receptors that regulate cell adhesion, migration and remodelling of the ECM (29-31). Additionally, ITGAV and ITGA6 were also identified as miR-25 predicted targets using miRDB (15) and microTCDS (16). Moreover integrin-transmembrane receptors regulate the activation of Rho-GTPases, RAC1 and CDC42 (32). Interestingly, our mRNA analysis **(Fig. 2B)** revealed that miR-25 significantly down-regulated CDC42 and its effector proteins CDC42BPA and CDC42EP2 and decreased mRNA of RAC1 **(Fig. 2 C,D,E and Fig. 2 F,G,H).** Additionally, our RT-qPCR analysis revealed that miR-25 could significantly decreased PIP5K1C, kinase involved in RAC1 signaling and predicted target of miR-25 in both cell lines **(Fig. 2 C,D,E and Fig. 2 F,G,H).**

Previously we have shown that ITGAV is required for the acquisition of a stem/progenitor phenotype (31). Additionally, ITGAV and ITGA6 are highly expressed in prostate progenitor cells and ITGA6 has been established as maker for progenitor cells in prostate and breast cancer. These results suggested a functional link between miR-25 and ITGAV and ITGA6 expression regulation in prostate cancer, for which no information is currently available.

miR-25 overexpression down-regulates α_v and α_6 integrins in human prostate cancer cell lines and selected ALDH^{high} subpopulation

To investigate the functional interaction between miR-25 and the predicted target genes we isolated ALDH^{high} and ALDH^{low} from PC-3M-Pro4Luc2 prostate cancer cell line by flow cytometry. As expected, the clonogenic and migratory potential of ALDH^{high} vs ALDH^{low} cells was higher (11) (**Suppl. Fig. 1B, C**). Furthermore, ITGAV and ITGA6 expression was also higher in ALDH^{high} vs ALDH^{low} cells as expected, thus confirming the inverse correlation with miR-25 expression (11) (**Suppl. Fig. 1D**). We used ITGA2, an established prostate cancer stem cell marker, as positive control and confirmed its increased expression in ALDH^{high} cells (5,11) (**Suppl. Fig. 1D**).

The functional interaction between miR-25 and ITGAV and ITGA6 expression in human prostate cancer cell lines and selected subpopulation of cells (ALDH^{high} stem/progenitors

and ALDH^{low} committed cells) was evaluated by transfection with 60nM of pre-miR-25 or pre-negative control sequence.

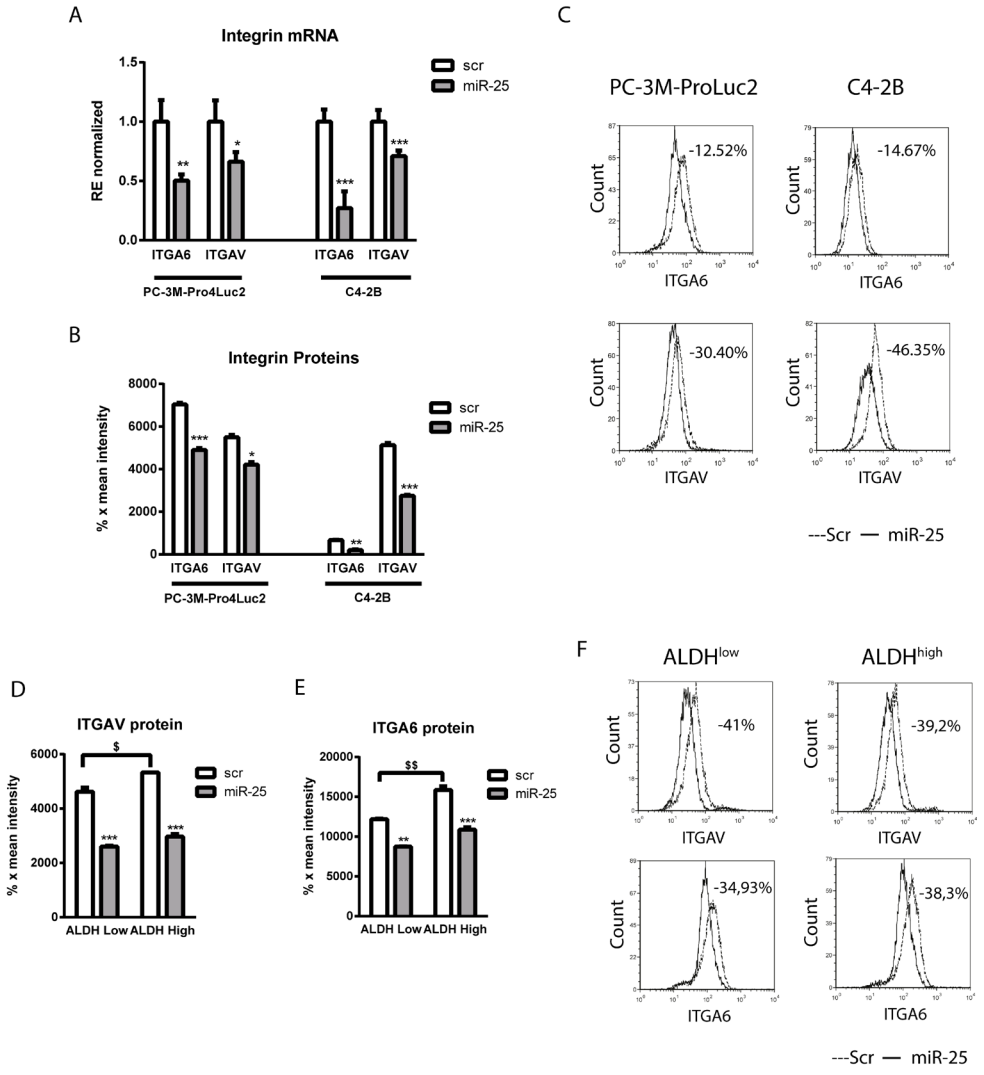

Figure 3. miR-25 overexpression decreases ITGAV and ITGA6 expression at mRNA and protein level in prostate cancer cells and selected ALDH^{high} subpopulation of cells. A) PC-3M-Pro4Luc2– and C4-2B–overexpressing miR-25; relative expression is compared with scramble negative control and all values were normalized to GAPDH; error bars, ±SEM (n = 3). **B**) mean intensity of ITGAV and ITGA6 fluorescence in PC-3M-Pro4Luc2– and C4-2B–overexpressing miR-25 compared with scramble-negative control determined by FACS analysis; error bars, ±SEM (n = 3). **C**) histogram of flow cytometric analysis of ITGAV and ITGA6 protein expression. Expression levels in cells overexpressing miR-25 (continued line)

are compared with scramble-negative control (dashed line). **D**) and **E**) mean intensity of ITGAV and ITGA6 fluorescence in $ALDH^{high}$- versus $ALDH^{low}$-overexpressing miR-25 compared with scramble-negative control determined by FACS analysis; error bars, ±SEM (n = 2). **F**) histogram of flow cytometric analysis of ITGAV and ITGA6 protein expression. Expression levels in $ALDH^{high}$ versus $ALDH^{low}$ subpopulation–overexpressing miR-25 (continued line) are compared with scramble-negative control (dashed line). * and $, P < 0.05; ** and $$, P < 0.01; ***, P < 0.001.

Overexpression of miR-25 significantly attenuated ITGAV and ITGA6 mRNA expression in PC-3M-Pro4Luc2 and C4-2B (ITGAV p-value = 0.05 and 0.001 respectively; ITGA6 p-value = 0.01 and 0.001 respectively) (**Fig. 3A**). Interestingly, forced overexpression of miR-25 also led to a significant reduction in ITGA5 expression in both cell lines (p-value= 0.01 and 0.001 respectively) and reduced levels of ITGA3, ITGB1 and ITGB4 in C4-2B (p-value= 0.01, 0.001 and 0.05 respectively). (**Suppl. Fig. 1E,F and Fig. 2B,C,D,E,F,G,H**). As expected, no consistent inhibitory effect was observed on ITGA2 expression.
Strikingly, upon transfection of PC-3M-Pro4Luc2 and C4-2B cells with pre-miR-25 (or pre-negative control) for 72 hours ITGAV and ITGA6 protein expression were also significantly down-regulated not only in the bulk cell lines (**Fig. 3B, C**) but also in selected $ALDH^{low}$ and highly aggressive $ALDH^{high}$ subpopulation of stem/progenitor cells transfected with pre-miR-25 (or pre-negative control) after viable cell sorting (**Fig. 3D, E**, **F)**.

miR-25 overexpression decreases migration of metastasis-initiating human prostate cancer cells and affects cytoskeleton dynamics

Prostate cancer cell migration in both PC-3M-Pro4Luc2 and C4-2B cells was significantly attenuated upon miR-25 overexpression (PC-3M-Pro4Luc2, 88% decrease, p-value= 0.001; C4-2B, 49% decrease, p-value=0.01 after 72 hrs) (**Fig. 4 A, B**).
Strikingly, miR-25 was able to strongly and significantly reduce migration also in selected highly migratory $ALDH^{high}$ subpopulation of stem/progenitor-like cells transfected after viable cell sorting (P<0.001) **(Fig. 4 C,D)**.
In contrast to migration, cell proliferation was not affected by forced miR-25 overexpression compared to the scrambled negative control sequence (**Suppl. Fig. 2A, B**). miR-25 also induced a switch to a less invasive phenotype characterized by a dramatic change in cell morphology (**Suppl. Fig. 2C**). Phalloidin staining revealed an almost complete loss of actin filopodia and cytoskeletal reorganization associated with a strong decrease in the average F-actin fluorescence (p-value= 0.01) (**Fig. 4E, F**). Additionally, migration was monitored in $ALDH^{high}$ and $ALDH^{low}$ subpopulation 4 days after sorting (i.e. 72 hours after transfection of selected subpopulation) and confirmed significantly higher conserved migratory potential in $ALDH^{high}$ cells compared to $ALDH^{low}$ (**Fig. 4 G, H**). Taken together these results suggest a critical role of miR-25 in the

regulation of an invasive phenotype by modulating cytoskeletal integrity, organization and motility in humane prostate cancer cell lines and selected aggressive tumor- and metastasis-initiating ALDH^{high} subpopulation (11).

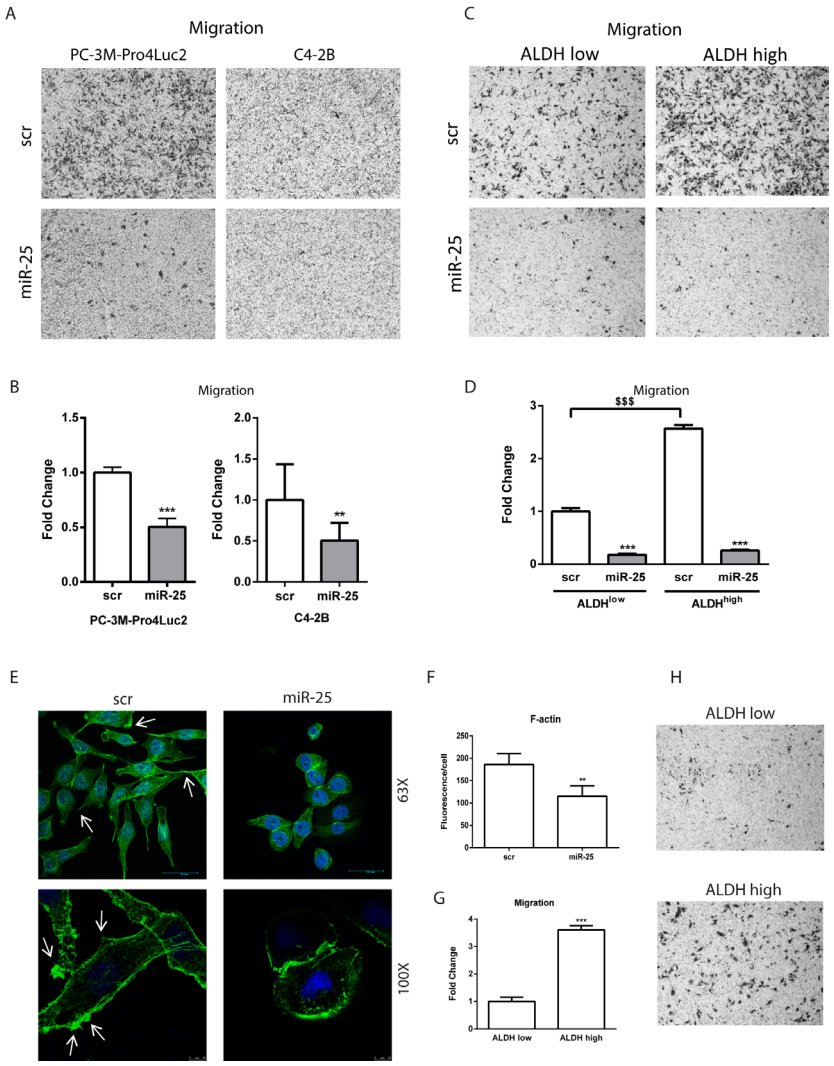

Figure 4. miR-25 overexpression affect cell morphology and decreases migration in prostate cancer cells and selected ALDH^{high} subpopulation of cells. A) representative images of PC-3M-Pro4Luc2 and C4-2B migrating in Transwell chambers after transfection with pre–miR-25 and prenegative control. **B**) mean number of migrated PC-3M-Pro4Luc2 and C4-2B cells per field transfected with scramble-negative control and pre–miR-25; error bars, ±SEM (n = 2). **C**) representative images of ALDH^{high} and ALDH^{low} subpopulation of cells migrating in Transwell chambers after transfection with pre–miR-25 and prenegative control; error bars, ±SEM (n = 2). **D**) mean number of migrated ALDH^{high} and

$ALDH^{low}$ subpopulation of cells per field transfected with scramble-negative control and pre–miR-25; error bars, ±SEM (n = 2). **E**) representative confocal images of PC-3M-Pro4Luc2 transfected with pre–miR-25 and prenegative control stained for F-actin with phalloidin (green) and nuclei with TO-PRO (blue). **F**) corrected total cell fluorescent of PC-3M-Pro4Luc2 transfected with scramble and pre–miR-25 measured with ImageJ and calculated as (integrated density − (area of selected cells × mean fluorescence of background readings)); error bars, ±SEM (n = 3 measurements). **G**) and **H**) mean number of migrated $ALDH^{high}$ and $ALDH^{low}$ subpopulation of cells per field and representative images of the $ALDH^{high}$ and $ALDH^{low}$ subpopulation of cells migrating in Transwell chambers; error bars, ±SEM (n = 2). **, P < 0.01; *** and $$$, P < 0.001.

The miR-25 induced change to a less invasive phenotype does not coincide with major changes in the expression of epithelial markers, suggesting that the observed morphological changes are most likely due to altered integrin expression as we demonstrated previously for α_v-integrins (31) (**Suppl. Fig. 2D, E**).

miR-25 directly targets pro-invasive α_6- and α_v-integrins

Next we investigated the putative direct functional interaction between miR-25 and its predicted ITGA6 and ITGAV target genes. For this we cloned 497 bp and 485 bp nucleotide sequences corresponding to a portion of the 3' UTR of ITGA6 and ITGAV respectively, including the conserved predicted binding site (seed sequence) for miR-25, downstream of the *firefly* luciferase2 sequence in a pGL4.10 vector background (see Materials & Methods) **(Fig. 5A)**.

To achieve high expression of the reporter system a 1184bp sequence corresponding to human elongation factor 1α (hEF1α) promoter was inserted into the multiple cloning site (MCS) of the pGL4.10 upstream to the luciferase2 sequence. The reporter constructs, containing mutant miR-25 binding site in the 3' UTR of the descripted genes, were also generated and used as a control. Transfection of pre-miR-25 resulted in a significant reduction of luciferase activity in the wild-type but not in the mutant 3' UTR of the ITGA6 and ITGAV genes (p-value= 0.05 for both genes) (**Fig. 5B, C**). These results, combined with the transcriptional and translational analysis described above, show for the first time that miR-25 directly targets ITGA6 and ITGAV expression.

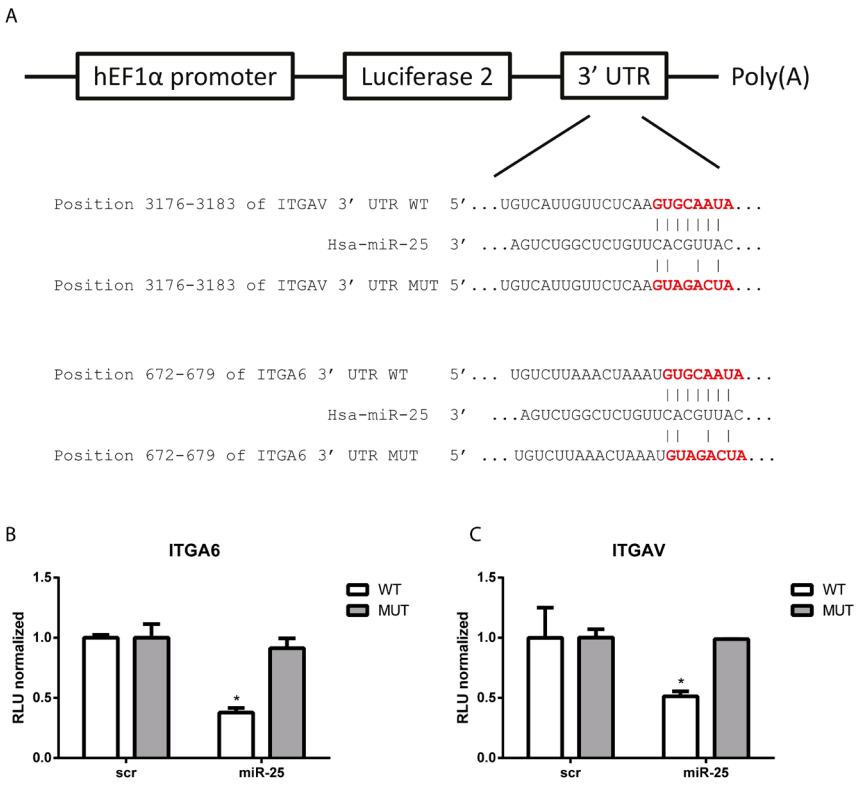

Figure 5. miR-25 directly regulates ITGAV and ITGA6. A) portion of 3′-UTR of ITGAV or ITGA6 containing the miR-25 predicted–binding site was cloned in PGL4-basic vector modified with hEF1α promoter. Scramble-negative control or pre–miR-25 was cotransfected with WT or MUT construct for ITGA6 (**B**) or ITGAV (**C**) together with CAGGS-renilla plasmid. RLU is calculated as ratio luciferase/renilla and normalized for scramble-negative control; error bars, ±SEM (n = 3). *, P < 0.05.

miR-25 inhibits distant metastasis of human prostate cancer cells in zebrafish

To investigate the ability of miR-25 to interfere with migration and invasion in the intact organism PC-3M-Pro4 prostate cancer cells, that stably express the NIRF protein mCherry, were injected into the circulatory system of zebrafish embryos and their tumor extravasation and distant metastasis formation was examined (33). The embryonic vascular system of zebrafish is fully functional and allows efficient detection of extravasating tumor cells (34). In addition, in the Tg(mpo:GFP)i114, the embryos are transparent and the immune system is not fully developed permitting successful xenotransplantation of human tumor cells (22). This makes the zebrafish model system highly appropriate for observing interaction between tumor cells and vasculature at the single cell level (35). We transfected PC-3M-Pro4mCherry cells to overexpress pre-miR-25

(or pre-negative control) and inoculated the cancer cells into the duct of Cuvier (DoC) of 2-day-old zebrafish embryos (100 embryos injected per group) (33). Disseminated cells were arrested in the host vasculature in the first hours, and extravasation was detected from 12hpi (hours post implantation). Perivascular tumor cells were observed in multiple foci, including the optic veins, the inter-segmental vessels, the dorsal aorta and the caudal vein. However, exclusively at the posterior ventral end of the tissue caudal hematopoietic (CHT, as indicated in **Fig. 6**) in the tail, perivascular tumor cells were able to invade into the neighboring tail fin. At day 1 post-implantation (1 dpi) miR-25 overexpression caused a robust and significant reduction in the distal colonization and invasion from CHT into the tail fin compared to the scramble control cells (**Fig. 6A**). miR-25 was able to completely abolish invasion which was detected in 20% of the embryos injected with cells transfected with pre-negative control. At day 2 post-implantation (2 dpi), 40% of embryos injected with cells overexpressing the negative control showed invasion from CHT, compared to 20% of embryos injected with cells overexpressing miR-25 (**Fig. 6 B, C**). In addition, miR-25 was able to significantly reduce the number of tumorigenic foci/embryo at 1 dpi while no significant difference was measured at 2 dpi (**Fig. 7 A, B, C**).

Taken together, our experimental metastasis data support the findings *in vitro* and indicate that miR-25 negatively regulates the acquisition of an invasive, metastatic phenotype in human prostate cancer cells.

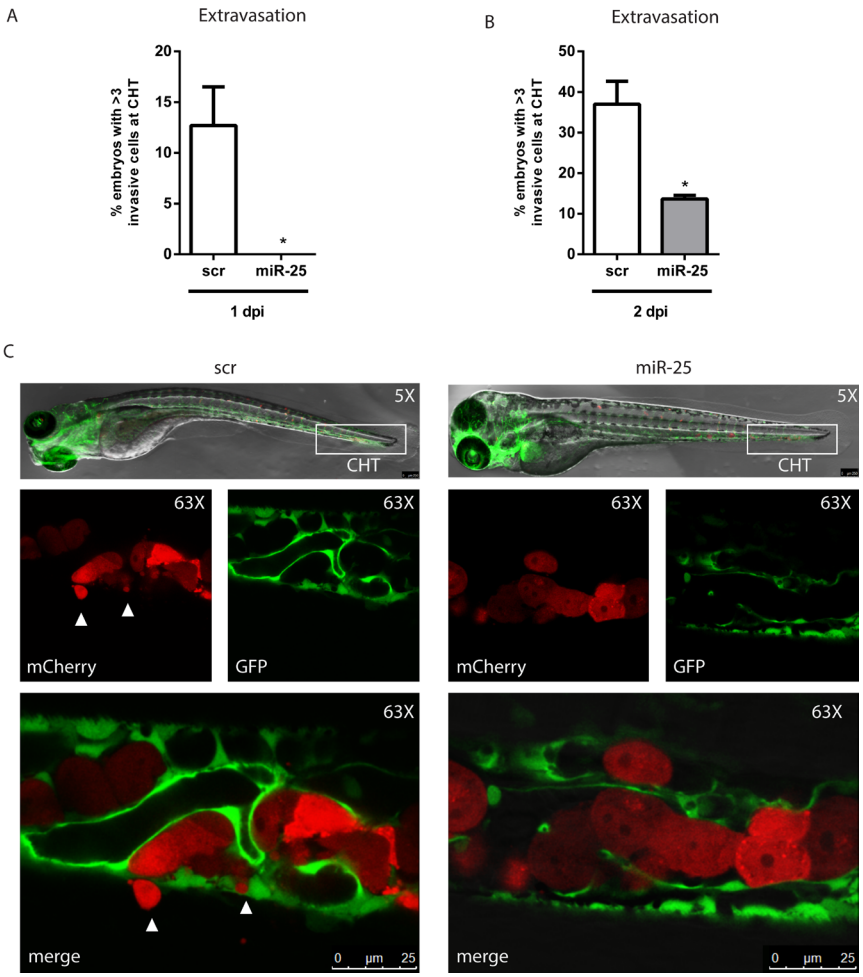

Figure 6. miR-25–overexpressing cells injected in zebrafish circulation show reduced extravasation. Of note, 100 embryos per group were injected and the percentage of embryos with invasion at CHT (invasion defined as >3 cells extravasating/embryo) was counted at day 1 post-injection (1 dpi; **A**) and day 2 postinjection (2 dpi; **B**); error bars, ±SEM (n = 2 experiments). **C**) representative confocal images of zebrafish embryos injected with PC-3M-Pro4mCherry cells overexpressing miR-25 or negative control. Cells overexpressing miR-25 were lodged into circulation, whereas cells overexpressing negative control started to show extravasation, full out of CHT and from CHT into the neighboring tail fin at 1 dpi. *, $P < 0.05$.

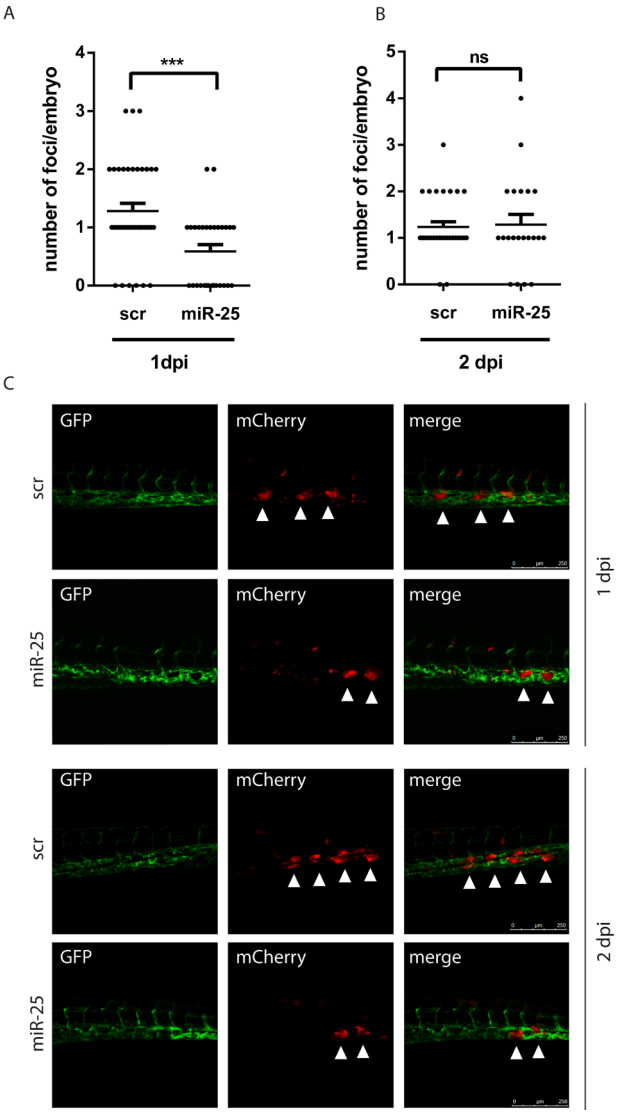

Figure 7. miR-25–overexpressing cells injected in zebrafish circulation show reduced tumor foci (colonization). A) number of tumor foci is reduced in embryos injected with cells overexpressing miR-25 compared with negative control at 1 day post-injection (1 dpi). **B**) no difference in the number of foci from embryos injected with cells overexpressing miR-25 and scr was measured at day 2 post-injection (2 dpi). 100 embryos per group were injected; error bars indicate ±SEM (n = 2 experiments). **C**) representative confocal images of zebrafish embryos injected with PC-3M-Pro4mCherry cells overexpressing miR-25 or negative control at 1 dpi and 2 dpi. ***, $P < 0.001$.

Discussion

In this study, miR-25 was identified as an important regulator of the invasive program in non-transformed and malignant human prostate epithelial tissues. In human prostate cancer cell lines and patient-derived primary prostate tumors, miR-25 expression was low/absent in the $\alpha2\beta1^{hi}$ /$CD133^{+}$ (SC) cell subpopulation but its expression steadily increased during differentiation to $\alpha2\beta1^{hi}$ /$CD133^{-}$ (TA) cells and $\alpha2\beta1^{low}$ (CB) cells committed for terminal differentiation (12). Here we identified, for the first time, the pro-invasive α_v- and α_6-integrins as functional target genes of miR-25. Forced overexpression of miR-25 in human prostate cancer cells and in highly metastatic and aggressive subpopulation of cells ($ALDH^{high}$) leads to a strong and significant decline in α_v- and α_6-integrin driven invasive behavior *in vitro* and blockage of metastatic colonization in the intact organism.

Consistent with these observations, overexpression of miR-25 decreased migration and strongly affected cell morphology of prostate cancer cells through its direct effect on the cytoskeletal arrangement and dynamics. miR-25 may, therefore, represent one of the key regulators of the invasive program in the human prostate epithelium, in particular in the maintenance of an aggressive phenotype in human prostate cancer “driver” subpopulation of stem/progenitor-like cells.
The results from this study support the notion that the stem/progenitor subpopulation in human prostate cancer displays increased clonogenic, migratory properties *in vitro* and stronger tumor- and metastasis-initiating properties in preclinical *in vivo* models (11).
miR-25 is part of the miR-106b-25 cluster which was previously reported to be up-regulated in primary tumors and distant metastasis in prostate cancer (36-40). A likely explanation for these apparent contradictory observations is that cancer cell lines and bulk tumor tissues are not homogeneous and consist of a mixture of heterogeneous subpopulations of cells (2). The findings reported here suggest that cellular heterogeneity may limit the appropriate interpretation of RNA expression-based analysis data obtained from *bulk* tissues. The cellular composition and proportion of $\alpha2\beta1^{hi}$/$CD133^{+}$, $\alpha2\beta1^{hi}$/$CD133^{-}$ and $\alpha2\beta1^{low}$, also referred to as stem-like cells (SC), transit amplifying cells (TA) and committed basal cells (CB) (12) in the normal prostate epithelium vs prostate cancer epithelium is indeed generally very different (5). For instance, the “driver” stem/progenitor subpopulation in the human prostate often represents only 0.02% of all prostate epithelial cells (5,41). The increase in absolute expression levels of miR-25 in bulk tissues during prostate cancer progression may,

therefore, be indicative of an increase in the proportion of more differentiated, less invasive, miR-25^{high} luminal epithelial cells.

Here we focused primarily on the differential miR expression in α2β1^{hi} /CD133^{+} cells as a cellular subpopulation that "drives" tumorigenesis and metastasis (14). Our findings, indeed, confirmed that miR-25 is overexpressed in hormone-naive and castration-resistant prostate cancer as previously reported by others (38,42). Intriguingly, we found that -despite the previously observed upregulation of miR-25 in bulk prostate cancer tissues (38) the expression of miR-25 in the α2β1^{hi} /CD133^{+} cells isolated from prostate cancer patients matched its expression in the tumor- and metastasis-initiating ALDH^{high} prostate cancer stem/progenitor subpopulation (11). Our analysis on the α2β1^{hi} /CD133^{+}, α2β1^{hi} /CD133^{-} and α2β1^{low} cell compartment enriched from primary prostate cancer samples supports the notion that miR-25 is down-regulated in the stem/progenitor cell compartment and that its expression steadily increases during differentiation. Consistent with our findings, the expression of the miR-106b-25 cluster appears to mediate neuronal differentiation of adult neural stem/progenitor cells and, interestingly, induction of miR-106b-25 in hypoxic conditions was recently linked to increased expression of neuronal markers in prostate cancer cell lines (43,44).

Thus, our work and these results suggest that lower miR-25 expression is needed to maintain stem/progenitor phenotype and its increase is associated with cellular differentiation.

In line with the miR-25 data presented in this study, we previously found that α_v-integrins play a pivotal role in the acquisition of a migratory stem/progenitor phenotype, tumorigenicity and the formation of distant bone metastasis *in vivo* (31,45). Moreover, $\alpha_6\beta_4$ integrin expression has already been associated with prostate cancer invasion, metastasis and disease progression (46-48). In addition, integrins provide a structural link between F-actin and the extracellular matrix and contribute to formation of focal adhesion points (49). Our confocal analysis showed that overexpression of miR-25 dramatically affected cell morphology and impaired F-actin polymerization, reducing focal adhesion sites. It seems, therefore that miR-25 is a key player in the organization of the F-actin and exerts a crucial role in the regulation of an aggressive and migratory phenotype with its direct effect on integrin expression. In addition, organization of F-actin is linked to activation of integrin-transmembrane receptor which regulates the activation of Rho-GTPases, RAC1 and CDC42 (32). Aberrant migration and invasion of cancer cells are key components of their invasive-metastatic phenotype. Individual tumor cells with an elongated, morphology like PC-3M-Pro4Luc2, often migrate in a "mesenchymal manner", which requires activation of RAC1, decreased by miR-25 (28). In contrast, single tumor cells with a less mesenchymal phenotype, like C4-2B, migrate with an "amoeboid mode" which requires signalling of CDC42, significantly down-

regulated after miR-25 overexpression (28). Our *in silico* analysis, revealed that PIP5K1C and PIP4K2C, kinases involved RAC1 signalling, are also predicted target of miR-25. In addition, our transcriptional analysis indicated that miR-25 down-regulates CDC42 mRNA together with CDC42BPA and CDC42EP2 mRNA (CDC42 effector proteins). This information combined with the evidence provided by our mRNA and protein analysis on integrin expression in bulk cell lines and selected subpopulation of highly metastatic cells ($ALDH^{high}$), suggest that miR-25 could be a central player in F-actin organization and cytoskeletal dynamics. However, the observed miR-25- induced loss of a migratory phenotype, confirmed in selected $ALDH^{high}$ subpopulation of stem/progenitor-like cells, could not be fully explained by the acquisition of more epithelial characteristics (or blockage of EMT-like processes), despite the fact that E-Cadherin is a validated target gene of miR-25 (50).

Consistent with our *in vitro* observations, complete blocking of metastasis by prostate cancer cells overexpressing miR-25 at 1 dpi and a strong reduction at 2 dpi was found in embryonic zebrafish model (33). These observations indicate that the morphological alterations produced by miR-25 disrupt extravasation and colonisation at distant sites *in vivo.*

In conclusion, we identified -for the first time- a direct functional interaction between miR-25 and integrins as key regulators of prostate cancer invasiveness and metastasis. Our *in vitro* and *in vivo* data indicate that miR-25 can have a suppressor role in aggressive human prostate cancer cells (cell lines and selected subpopulation of $ALDH^{high}$ cells) by blocking invasion, and metastasis by promoting prostate epithelial differentiation and by disrupting. From a therapeutic perspective, miR-25 seems an interesting small molecule for specific targeting of stem/progenitor-like cells in aggressive human prostate cancer.

Acknowledgements

We would like to thank Guido de Roo from the Flow cytometry facility (Dept. of Hematology, LUMC, The Netherlands) and Dr. Twan de Vries (Dept. of Cardiology, LUMC, The Netherlands) for kindly providing construct with hEF1α promoter. We also would like to thank Chris van der Bent and Hetty Sips (Dept. of Endocrinology, LUMC, The Netherlands) for help and technical support. The research leading to these results has received funding from the FP7 Marie Curie ITN under grant agreement n°264817 - BONE-NET (EZ) and n°238278 - PRONEST (JR). This project receives also additional support from Prostate Action UK (EZ, JR) and from the Dutch Cancer Society (UL-2011-4930) (GvdH).

REFERENCES

1. Jemal A, Center MM, DeSantis C, Ward EM. Global patterns of cancer incidence and mortality rates and trends. Cancer Epidemiol Biomarkers Prev 2010;19(8):1893-907.
2. Shackleton M, Quintana E, Fearon ER, Morrison SJ. Heterogeneity in cancer: cancer stem cells versus clonal evolution. Cell 2009;138(5):822-9.
3. Dean M, Fojo T, Bates S. Tumour stem cells and drug resistance. Nat Rev Cancer 2005;5(4):275-84.
4. Maitland NJ, Collins AT. Prostate cancer stem cells: a new target for therapy. J Clin Oncol 2008;26(17):2862-70.
5. Collins AT, Berry PA, Hyde C, Stower MJ, Maitland NJ. Prospective identification of tumorigenic prostate cancer stem cells. Cancer research 2005;65(23):10946-51.
6. Reya T, Morrison SJ, Clarke MF, Weissman IL. Stem cells, cancer, and cancer stem cells. Nature 2001;414(6859):105-11.
7. Calin GA, Croce CM. MicroRNA signatures in human cancers. Nat Rev Cancer 2006;6(11):857-66.
8. Bartel DP. MicroRNAs: target recognition and regulatory functions. Cell 2009;136(2):215-33.
9. Mitchell PS, Parkin RK, Kroh EM, Fritz BR, Wyman SK, Pogosova-Agadjanyan EL, et al. Circulating microRNAs as stable blood-based markers for cancer detection. Proc Natl Acad Sci U S A 2008;105(30):10513-8.
10. Bryant RJ, Pawlowski T, Catto JW, Marsden G, Vessella RL, Rhees B, et al. Changes in circulating microRNA levels associated with prostate cancer. Br J Cancer 2012;106(4):768-74.
11. van den Hoogen C, van der Horst G, Cheung H, Buijs JT, Lippitt JM, Guzman-Ramirez N, et al. High aldehyde dehydrogenase activity identifies tumor-initiating and metastasis-initiating cells in human prostate cancer. Cancer research 2010;70(12):5163-73.
12. Rane JK, Scaravilli M, Ylipaa A, Pellacani D, Mann VM, Simms MS, et al. MicroRNA expression profile of primary prostate cancer stem cells as a source of biomarkers and therapeutic targets. Eur Urol 2015;67(1):7-10.
13. Collins AT, Habib FK, Maitland NJ, Neal DE. Identification and isolation of human prostate epithelial stem cells based on alpha(2)beta(1)-integrin expression. J Cell Sci 2001;114(Pt 21):3865-72.
14. Richardson GD, Robson CN, Lang SH, Neal DE, Maitland NJ, Collins AT. CD133, a novel marker for human prostatic epithelial stem cells. J Cell Sci 2004;117(Pt 16):3539-45.
15. Wang X. miRDB: a microRNA target prediction and functional annotation database with a wiki interface. Rna 2008;14(6):1012-7.
16. Paraskevopoulou MD, Georgakilas G, Kostoulas N, Vlachos IS, Vergoulis T, Reczko M, et al. DIANA-microT web server v5.0: service integration into miRNA functional analysis workflows. Nucleic acids research 2013;41(Web Server issue):W169-73.
17. Huang da W, Sherman BT, Lempicki RA. Systematic and integrative analysis of large gene lists using DAVID bioinformatics resources. Nat Protoc 2009;4(1):44-57.
18. Huang da W, Sherman BT, Lempicki RA. Bioinformatics enrichment tools: paths toward the comprehensive functional analysis of large gene lists. Nucleic Acids Res 2009;37(1):1-13.
19. Kanehisa M, Goto S. KEGG: kyoto encyclopedia of genes and genomes. Nucleic Acids Res 2000;28(1):27-30.
20. Stoletov K, Montel V, Lester RD, Gonias SL, Klemke R. High-resolution imaging of the dynamic tumor cell vascular interface in transparent zebrafish. Proc Natl Acad Sci U S A 2007;104(44):17406-11.
21. Lawson ND, Weinstein BM. In vivo imaging of embryonic vascular development using transgenic zebrafish. Dev Biol 2002;248(2):307-18.

22. Haldi M, Ton C, Seng WL, McGrath P. Human melanoma cells transplanted into zebrafish proliferate, migrate, produce melanin, form masses and stimulate angiogenesis in zebrafish. Angiogenesis 2006;9(3):139-51.
23. Ginestier C, Hur MH, Charafe-Jauffret E, Monville F, Dutcher J, Brown M, et al. ALDH1 is a marker of normal and malignant human mammary stem cells and a predictor of poor clinical outcome. Cell Stem Cell 2007;1(5):555-67.
24. Douville J, Beaulieu R, Balicki D. ALDH1 as a Functional Marker of Cancer Stem and Progenitor Cells. Stem Cells and Development 2009;18(1):17-25.
25. Kroon P, Berry PA, Stower MJ, Rodrigues G, Mann VM, Simms M, et al. JAK-STAT blockade inhibits tumor initiation and clonogenic recovery of prostate cancer stem-like cells. Cancer research 2013;73(16):5288-98.
26. Lewis BP, Burge CB, Bartel DP. Conserved seed pairing, often flanked by adenosines, indicates that thousands of human genes are microRNA targets. Cell 2005;120(1):15-20.
27. Kuhn AR, Schlauch K, Lao R, Halayko AJ, Gerthoffer WT, Singer CA. MicroRNA expression in human airway smooth muscle cells: role of miR-25 in regulation of airway smooth muscle phenotype. Am J Respir Cell Mol Biol 2010;42(4):506-13.
28. Gadea G, Sanz-Moreno V, Self A, Godi A, Marshall CJ. DOCK10-mediated Cdc42 activation is necessary for amoeboid invasion of melanoma cells. Curr Biol 2008;18(19):1456-65.
29. Hynes RO. Integrins: bidirectional, allosteric signaling machines. Cell 2002;110(6):673-87.
30. Legate KR, Wickstrom SA, Fassler R. Genetic and cell biological analysis of integrin outside-in signaling. Genes Dev 2009;23(4):397-418.
31. van den Hoogen C, van der Horst G, Cheung H, Buijs JT, Pelger RC, van der Pluijm G. Integrin alphav expression is required for the acquisition of a metastatic stem/progenitor cell phenotype in human prostate cancer. Am J Pathol 2011;179(5):2559-68.
32. Huveneers S, Danen EH. Adhesion signaling - crosstalk between integrins, Src and Rho. J Cell Sci 2009;122(Pt 8):1059-69.
33. Drabsch Y, He S, Zhang L, Snaar-Jagalska BE, Ten Dijke P. Transforming growth factor-beta signalling controls human breast cancer metastasis in a zebrafish xenograft model. Breast Cancer Res 2013;15(6):R106.
34. Isogai S, Lawson ND, Torrealday S, Horiguchi M, Weinstein BM. Angiogenic network formation in the developing vertebrate trunk. Development 2003;130(21):5281-90.
35. Stoletov K, Kato H, Zardouzian E, Kelber J, Yang J, Shattil S, et al. Visualizing extravasation dynamics of metastatic tumor cells. J Cell Sci 2010;123(Pt 13):2332-41.
36. Hudson RS, Yi M, Esposito D, Glynn SA, Starks AM, Yang Y, et al. MicroRNA-106b-25 cluster expression is associated with early disease recurrence and targets caspase-7 and focal adhesion in human prostate cancer. Oncogene 2013;32(35):4139-47.
37. Poliseno L, Salmena L, Riccardi L, Fornari A, Song MS, Hobbs RM, et al. Identification of the miR-106b~25 microRNA cluster as a proto-oncogenic PTEN-targeting intron that cooperates with its host gene MCM7 in transformation. Sci Signal 2010;3(117):ra29.
38. Ambs S, Prueitt RL, Yi M, Hudson RS, Howe TM, Petrocca F, et al. Genomic profiling of microRNA and messenger RNA reveals deregulated microRNA expression in prostate cancer. Cancer research 2008;68(15):6162-70.
39. Szczyrba J, Loprich E, Wach S, Jung V, Unteregger G, Barth S, et al. The microRNA profile of prostate carcinoma obtained by deep sequencing. Mol Cancer Res 2010;8(4):529-38.
40. Martens-Uzunova ES, Jalava SE, Dits NF, van Leenders GJ, Moller S, Trapman J, et al. Diagnostic and prognostic signatures from the small non-coding RNA transcriptome in prostate cancer. Oncogene 2012;31(8):978-91.
41. Polson ES, Lewis JL, Celik H, Mann VM, Stower MJ, Simms MS, et al. Monoallelic expression of TMPRSS2/ERG in prostate cancer stem cells. Nature communications 2013;4:1623.

42. Volinia S, Calin GA, Liu CG, Ambs S, Cimmino A, Petrocca F, et al. A microRNA expression signature of human solid tumors defines cancer gene targets. Proc Natl Acad Sci U S A 2006;103(7):2257-61.
43. Liang H, Studach L, Hullinger RL, Xie J, Andrisani OM. Down-regulation of RE-1 silencing transcription factor (REST) in advanced prostate cancer by hypoxia-induced miR-106b~25. Exp Cell Res 2014;320(2):188-99.
44. Brett JO, Renault VM, Rafalski VA, Webb AE, Brunet A. The microRNA cluster miR-106b~25 regulates adult neural stem/progenitor cell proliferation and neuronal differentiation. Aging (Albany NY) 2011;3(2):108-24.
45. Birnie R, Bryce SD, Roome C, Dussupt V, Droop A, Lang SH, et al. Gene expression profiling of human prostate cancer stem cells reveals a pro-inflammatory phenotype and the importance of extracellular matrix interactions. Genome Biol 2008;9(5):R83.
46. Eaton CL, Colombel M, van der Pluijm G, Cecchini M, Wetterwald A, Lippitt J, et al. Evaluation of the Frequency of Putative Prostate Cancer Stem Cells in Primary and Metastatic Prostate Cancer. Prostate 2010;70(8):875-82.
47. Tantivejkul K, Kalikin LM, Pienta KJ. Dynamic process of prostate cancer metastasis to bone. Journal of Cellular Biochemistry 2004;91(4):706-17.
48. Ricci E, Mattei E, Dumontet C, Eaton CL, Hamdy F, van der Pluije G, et al. Increased Expression of Putative Cancer Stem Cell Markers in the Bone Marrow of Prostate Cancer Patients Is Associated With Bone Metastasis Progression. Prostate 2013;73(16):1738-46.
49. Cluzel C, Saltel F, Lussi J, Paulhe F, Imhof BA, Wehrle-Haller B. The mechanisms and dynamics of (alpha)v(beta)3 integrin clustering in living cells. J Cell Biol 2005;171(2):383-92.
50. Xu X, Chen Z, Zhao X, Wang J, Ding D, Wang Z, et al. MicroRNA-25 promotes cell migration and invasion in esophageal squamous cell carcinoma. Biochem Biophys Res Commun 2012;421(4):640-5.

SUPPLEMENTARY DATA

Table I. Real time-qPCR primers		
GENE	**Forward Primer**	**Reverse Primer**
ITGA2	TTTGGTAGTGTGCTGTGTTC	GACTCTTCCTTCCTCTTTCTTTAG
ITGA3	GCATCAACGTGACGAACACC	TCTGGTTCCGTTTGAAGGGG
ITGA5	AGTCCTCACTGTCCAGCTCA	GCTCAGTGGCTCCTTCTCTG
ITGA6	GCTGGTTATAATCCTTCAATATCAATTGT	TTGGGCTCAGAACCTTGGTTT
ITGAV	GCTGGACTGTGGAGAAGAC	AAGTGAGGTTCAGGGCATTC
ITGB1	AGCAACGGACAGATCTGCAA	GCTGGGGTAATTTGTCCCGA
ITGB3	GTCTGCCACAGCAGTGACTT	CTTGTAGCGGACACAGGAGA
ITGB4	CTGTGTGCACGAGGGACATT	AAGGCTGACTCGGTGGAGAA
CDH1	TTGACGCCGAGAGCTACAC	GACCGGTGCAATCTTCAAA
CDH2	CAGACCGACCCAAACAGCAAC	GCAGCAACAGTAAGGACAAACATC
VIM	CCAAACTTTTCCTCCCTGAACC	CGTGATGCTGAGAAGTTTCGTTGA
ZEB1	CCATATTGAGCTGTTGCCGC	GCCCTTCCTTTCCTGTGTCA
ZEB2	GACCTGGCAGTGAAGGAAAA	GGCACTTGCAGAAACACAGA
SNAIL1	ACCACTATGCCGCGCTCTT	GGTCGTAGGGCTGCTGGAA
SNAIL2	TGTGTGGACTACCGCTGC	TCCGGAAAGAGGAGAGAGG
PIP5K2C	CATGCATAGCAACCTCTCCA	ACTGACTCGGTACATCCCCA
PIP5K1C	CTGGAGGTACCGGACGAG	ACAGAACCTCTGTTGGGGC
RAC1	TCTCCAGGAAATGCATTGGT	CTGATGCAGGCCATCAAGT
CDC42EP2	GTCCAGCTCCTGAGACCTTG	TCACCGAGGGTTACTTGTCC
CDC42BPA	CATTCTCGAATACCTAGAATGGG	CAAAAGCTCCTCGACCAATC
CDC42	CCCGGTGGAGAAGCTGAG	CGCCCACAACAACACACTTA
TWIST	GCCGGAGACCTAGATGTCATT	TTTTAAAAGTGCGCCCCACG
GAPDH	GACAGTCAGCCGCATCTTC	GCAACAATATCCACTTTACCAGAG

Table II. Primers used for cloning and mutagenesis		
GENE	**Forward Primer**	**Reverse Primer**
3'UTR ITGAV WT	GCATATTCTAGACCTATGTGCAGCCACTACCC	GCATATGGCCGGCCTTCCAGCCTGAAATA CAATGC
3'UTR ITGA6 WT	GCATATTCTAGAACATCATGTGTTGGGGAAGG	GCATATGGCCGGCCAAAGTGATGACCTCCC ATGC
3'UTR ITGAV MUT	GAATCTTTGATGTTTTTTGTCATTGTTCTCAAGTAGA CTATAACAATGTAACCAAATCTAGATAATTTCAAA	TTTGAAATTATCTAGATTTGGTTACATTGTT ATAGTCTACTTGAGAACAATGACAAAAAAC ATCAAAGATTC
3'UTR ITGA6 MUT	CGGAAAGTGCTGTCTTAAACTAAATGTAGACTAGAAG GTGATGTTGCCATCC	GGATGGCAACATCACCTTCTAGTCTACATT TAGTTTAAGACAGCACTTTCCG

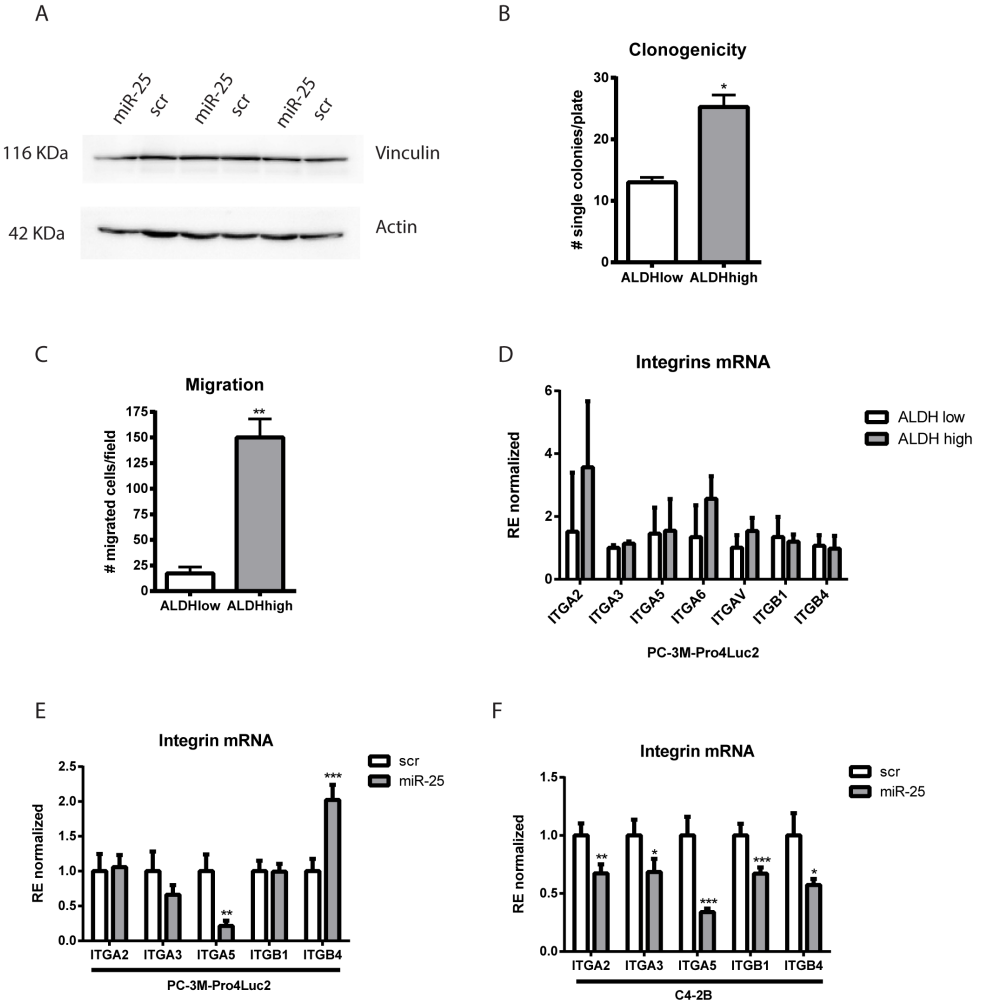

Supplementary Figure S1. ALDHhigh prostate cancer cells display enhanced colony formation and migration compared to ALDHlow cells. A) Western Blot analysis for Vinculin (VCL) expression after miR-25 transfection. No effect on protein is detected. **B**) Number of colonies per 96-well plate in single cell diluted culture after 2 weeks. **C**) Mean number of migrated ALDHhigh and ALDHlow PC-3M-Pro4Luc2 cells. Error bars indicate ±SEM **D**) qRT-PCR analysis on ITGA2, ITGA3, ITGA5, ITGA6, ITGAV, ITGAB1, ITGB4 on ALDHhigh VS ALDHlow PC-3M-Pro4Luc2 cells. ITGB3 displayed very low expression (ct > 35, data not shown). **E-F**) qRT-PCR analysis on ITGA2, ITGA3, ITGA5, ITGAB1, ITGB4 in PC-3M-Pro4Luc2 and C4-2B transfected with pre-miR-25 and negative control. ITGB3 displayed very low expression (ct > 35, data not shown). Error bars indicate ±SEM (n=3).

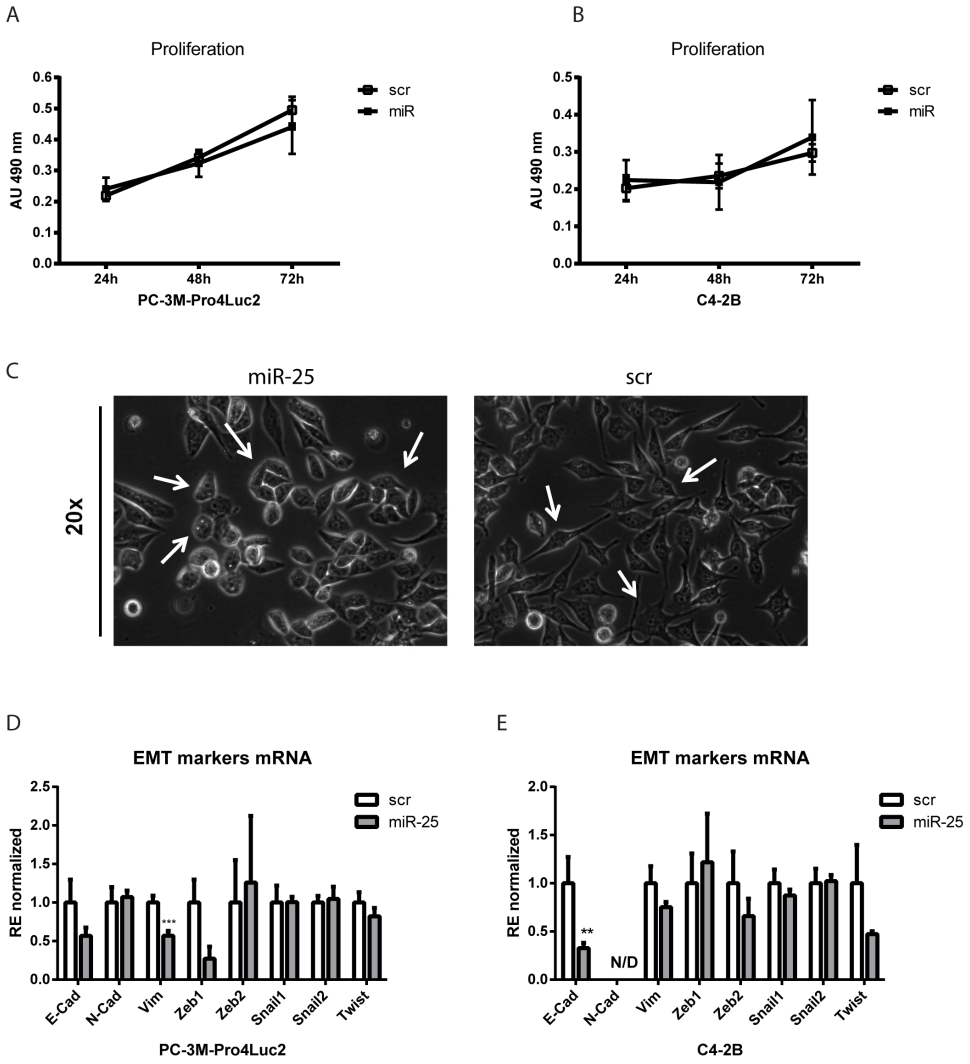

Supplementary Figure S2. miR-25 strongly changes cell morphology without affecting proliferation. A) MTS proliferation assay measured at 490nm 24-48-72 hours after miR-25 and control overexpression in PC-3M-Pro4Luc2 and **B**) C4-2B cells. **C**) Representative bright field picture of PC-3M-Pro4Luc2 cells overexpressing miR-25 and negative control 72 hours after transfection. miR-25 induces dramatic change in cell morphology. **D-E**) qRT-PCR on EMT markers (E-Cad, N-cad, Vim, Zeb1, Zeb2, Snail1, Snail2, Twist) in PC-3M-Pro4Luc2 and C4-2B respectively. Relative expression is compared to scramble negative control and all values were normalized to GAPDH. Error bars indicate ±SEM (n=3).